Improving teleportation fidelity in structured reservoirs

Yu-Xia Xie* and Xiao-Qiang Xi
School of Science, Xi'an University of Posts and Telecommunications, Xi'an 710121, China

Seeking flexible methods to control quantum teleportation in open systems is an important task of quantum communication. In this paper, we study how the super-Ohmic, Ohmic and sub-Ohmic reservoirs affect teleportation of a general one-qubit state. The results revealed that the structures of the reservoirs play a decisive role on quality of teleportation. Particularly, the fidelity of teleportation may be improved by the strong backaction of the non-Markovian memory effects of the reservoir. The physical mechanism responsible for this improvement are determined.

PACS numbers: 03.67.-a, 03.67.Hk, 03.65.Yz

arXiv:1211.2380v1 [quant-ph] 11 Nov 2012

I. INTRODUCTION

Since the seminal work of Bennett et al. [1], quantum teleportation undergoes rapid development both in the theory [2–7] and experiments [8–11]. Particularly, quantum teleportation via free-space channels over 97 kilometres [12] and 143 kilometres [13] have been experimentally realized recently by two research groups leaded by Pan and Zeilinger, respectively. These finding rekindled the dream of people on constructing ultra-long-distance quantum communication networks on a global scale. To make this dream come true, one needs to face many actual challenges. One such challenge is the decoherence of quantum states due to its inevitable interaction with the surroundings [14–16]. This unwanted interaction in most cases causes degradation of quantum correlations [17–19], and therefore limits the fidelity as well as the distance of quantum teleportation. Even for the simplest protocol of one-qubit teleportation [1], there are many processes that decoherence may be set in, e.g., the preparation and distribution processes of the shared quantum channels, the imperfect measurements of the information sender (Alice) and receiver (Bob). All these make it significant and vital to investigate resistance of a teleportation protocol under the influence of decoherence, and this subject has been studied by many authors from the perspective of both noise channels [20–26] and noisy operations [27, 28]. Particularly, it has been shown that although entanglement is the necessary resource for quantum teleportation, in general its magnitude is not proportional to the value of the teleportation fidelity [24–26].

In the present work, we study quantum teleportation of the single-qubit state in the bosonic structured reservoirs of the super-Ohmic, Ohmic and sub-Ohmic types [29]. Through simulating numerically the dynamical behaviors of the average teleportation fidelity, we show that the explicit form of the spectral density of the reservoir as well as the coupling strength between the channel and the reservoir have great impact on efficiency of quantum teleportation, and the quality of teleportation can be improved via the technique of reservoir engineering.

The structure of this paper is arranged as follows. In Section II we recall some basic formalism related to the fidelity of quantum teleportation, and detailed the methods for solving the equation of motion for the channel state. Then in Section III, we investigate resistance of quantum teleportation against decoherence induced by the super-Ohmic, Ohmic and sub-Ohmic reservoirs. Finally, Section IV is devoted to a summary.

II. THE FORMALISM

In this work we concentrate on efficiency of quantum teleportation for a general one-qubit state, with a two-qubit state ρ serving as the quantum channel. We suppose during the teleportation process, Alice performs only the Bell-basis measurement, while Bob is equipped to perform any unitary transformation, then the maximal average fidelity achievable can be evaluated as [30]

$$F_{\rm av} = \frac{1}{2} + \frac{1}{6}N(\rho), \tag{1}$$

where $N(\rho) = {\rm Tr}\sqrt{T^\dagger T}$, with T being the 3×3 positive matrix with elements t_{nm} related to the Bloch sphere representation of ρ below

$$\rho = \frac{1}{4}\sum_{n,m=0}^{3} t_{nm}\sigma_n \otimes \sigma_m, \tag{2}$$

with σ_0 being the 2×2 identity operator, $\sigma_{1,2,3}$ are the usual Pauli matrices, and $t_{nm} = {\rm Tr}(\rho\sigma_n\otimes\sigma_m)$.

To evaluate resistance of the teleportation protocol, we suppose the channel state consists of two identical qubits which coupled independently to their own reservoir, with the single "qubit+reservoir" Hamiltonian reads [31]

$$\hat{H} = \omega_0\sigma_+\sigma_- + \sum_k \omega_k b_k^\dagger b_k + \sum_k (g_k b_k \sigma_+ + {\rm H.c.}), \tag{3}$$

with ω_0 being the Bohr frequency of the two qubits, and the index k labels the reservoir field mode with frequency ω_k and the system-reservoir coupling strength g_k. Moreover, σ_+ (σ_-) are the usual Pauli raising (lowering) operator, while $b_k^\dagger$ (b_k) are the bosonic creation (annihilation) operator.

*Electronic address: yuxia1124@163.com

Under the assumption of zero-temperature reservoir and nullity of initial correlation between the qubit and the reservoir, the reduced density matrix $\rho^S(t)$ for qubit S ($S = A, B$) can be obtained as [31]

$$\rho^S(t) = \begin{pmatrix} \rho^S_{11}(0)|p(t)|^2 & \rho^S_{10}(0)p(t) \\ \rho^S_{01}(0)p^*(t) & 1-\rho^S_{11}(0)|p(t)|^2 \end{pmatrix}, \quad (4)$$

in the standard basis $\{|1\rangle, |0\rangle\}$, and $\rho^S_{ij}(0) = \langle i|\rho^S(0)|j\rangle$. The density matrix $\rho^S(t)$ depends solely on the function $p(t)$, whose explicit time dependence contains the information on the reservoir spectral density and the coupling constants. To be explicitly, we consider here the family of reservoir spectral densities given by [29]

$$J(\omega) = \sum_k |g_k|^2 \delta(\omega - \omega_k), \quad (5)$$

which simplifies to

$$J(\omega) = \eta \omega^s \omega_c^{1-s} e^{-\omega/\omega_c}, \quad (6)$$

in the continuum limit of reservoir modes $\sum_k |g_k|^2 \to \int d(\omega) J(\omega)$, with ω_c being the cutoff frequency and η the dimensionless coupling constant. They are related to the reservoir correlation time τ_B and the relaxation time τ_R by $\tau_B \simeq \omega_c^{-1}$ and $\tau_R \simeq \eta^{-1}$. By tuning the value of s, the spectral densities may be in the regime of sub-Ohmic ($0 < s < 1$), Ohmic ($s = 1$) or super-Ohmic ($s > 1$).

For this family of reservoir spectral densities, the function $p(t)$ obeys the following integro-differential equation [32]

$$\dot{p}(t) + i\omega_0 p(t) + \int_0^t p(t_1) f(t - t_1) dt_1 = 0, \quad (7)$$

where the kernel function $f(t-t_1) = \int d\omega J(\omega) e^{-i\omega(t-t_1)}$. After a straightforward algebra, Eq. (7) turns into

$$p(t) = p(0) - \int_0^t \left(i\omega_0 + \int_{t_1}^t f(t - t_1) dt \right) p(t_1) dt_1. \quad (8)$$

In this work we take $s = 1/2$, 1 and 3 as three examples of the sub-Ohmic, Ohmic, and super-Ohmic spectral densities. The kernel function can then be integrated as [6]

$$f(t - t_1) = \begin{cases} \dfrac{s!\eta\omega_c^2}{[1 + i\omega_c(t - t_1)]^{s+1}} & (s \in \mathbb{Z}), \\ \dfrac{\sqrt{\pi}\eta\omega_c^2 e^{-i\varpi}}{2[1 + \omega_c^2(t - t_1)^2]^{3/4}} & (s = 1/2), \end{cases} \quad (9)$$

where $s!$ is the factorial of s, and $\varpi = \frac{3}{2}\tan^{-1}[\omega_c(t-t_1)]$. With the help of Eq. (9), the function $p(t)$ in Eq. (8) can be solved numerically and the two-qubit density matrix $\rho(t)$ can be determined by the procedure of Ref. [33].

In fact, the equation of motion of qubit S can also be written in the following master equation form (by differentiating Eq. (4) with respect to time) of the form

$$\begin{aligned} \dot{\rho}^S(t) \;=\; & -i\frac{\Omega(t)}{2}[\sigma_+\sigma_-, \rho^S(t)] + \frac{\Gamma(t)}{2}[2\sigma_-\rho^S(t)\sigma_+ \\ & -\sigma_+\sigma_-\rho^S(t) - \rho^S(t)\sigma_+\sigma_-], \end{aligned} \quad (10)$$

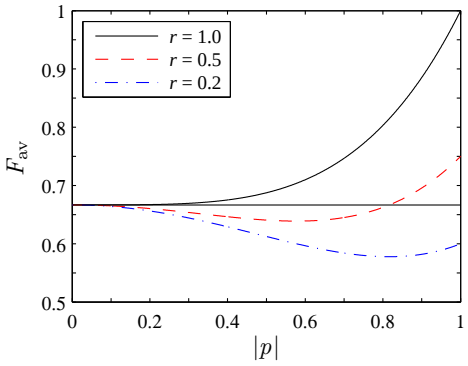

FIG. 1: (Color online) The $|p(t)|$ dependence of the average fidelity $F_{\rm av}$ with different mixing parameters of $\rho(0)$.

with the time-dependent decay rate $\Gamma(t)$ and Lamb shift $\Omega(t)$ given by [31]

$$\Gamma(t) = -2\mathrm{Re}\left[\frac{\dot{p}(t)}{p(t)}\right], \; \Omega(t) = -2\mathrm{Im}\left[\frac{\dot{p}(t)}{p(t)}\right]. \quad (11)$$

In general, the absolute values of $\Gamma(t)$ may be larger than unity. In the following, we define the normalized decay rate $\gamma(t) = \Gamma(t)/\Gamma_{\max}(t)$ for better visualizing the corresponding phenomena, where the maximum is taken over the entire time region for fixed η and ω_c.

III. AVERAGE FIDELITY DYNAMICS

Here we suppose the channel state is prepared initially in the Werner-like state [34]

$$\rho(0) = r|\Psi\rangle\langle\Psi| + \frac{1-r}{4}\mathbb{I}, \quad (12)$$

where $|\Psi\rangle = (|00\rangle + |11\rangle)/\sqrt{2}$. $\rho(0)$ is entangled if $1/3 < r \leqslant 1$ and separable if $0 \leqslant r \leqslant 1/3$. For this kind of $\rho(0)$, we have

$$N(\rho) = (r+1)|p(t)|^4 + 2(r-1)|p(t)|^2 + 1, \quad (13)$$

therefore the average teleportation fidelity $F_{\rm av}$ is determined by the absolute values of $p(t)$, and this applies to all kinds of reservoir spectral densities with the Hamiltonian model of Eq. (3).

By combining Eqs. (1) and (13), one can identify three different types of behavior of the $|p|$ dependence of $F_{\rm av}$ (see, Fig. 1), which depend on the values of the mixing parameter r: (i) for $r = 1$, $F_{\rm av}$ decays monotonically with the decrease of $|p|$ and arrives at the classical limiting value of $2/3$ when $|p| = 0$; (ii) for $1/3 < r < 1$, $F_{\rm av}$ first decays with the decrease of $|p|$, and then increase with the decrease of $|p|$ after the critical point $|p|_c^2 = (1-r)/(1+r)$, and $F_{\rm av}$ is larger than $2/3$ only when $|p|^2 > 2|p|_c^2$; (iii) for $0 \leqslant r \leqslant 1/3$, although $F_{\rm av}$ still decays with the decrease of $|p|$, and increase with the decrease of $|p|$ after $|p| > |p|_c$, its value cannot exceed $2/3$.

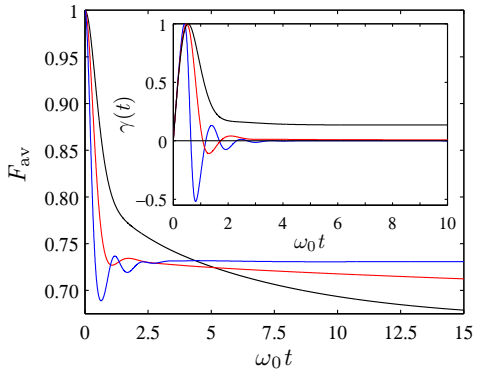

FIG. 2: (Color online) Average fidelity $F_{\rm av}$ versus $\omega_0 t$ in the super-Ohmic reservoir with $\omega_c = \omega_0$, $r = 1$, and $\eta = 0.15$ (black), 0.35 (red), 0.9 (blue). The inset shows behaviors of the corresponding normalized decay rates $\gamma(t)$.

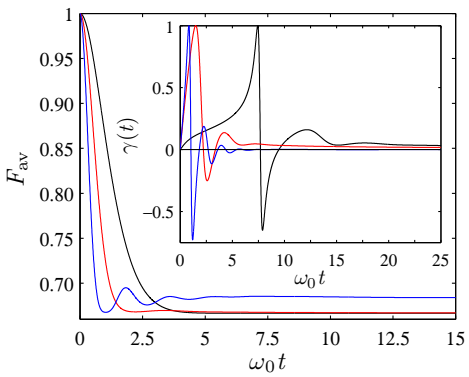

FIG. 3: (Color online) Average fidelity $F_{\rm av}$ versus $\omega_0 t$ in the Ohmic reservoir with $\omega_c = \omega_0$, $r = 1$, and $\eta = 0.3$ (black), 0.9 (red), 2.7 (blue). The inset shows behaviors of the corresponding normalized decay rates $\gamma(t)$.

In Fig. 2 we display dynamical behaviors of the average teleportation fidelity $F_{\rm av}$ for the case of super-Ohmic reservoir with the cutoff frequency $\omega_c = \omega_0$, mixing parameter $r = 1$ and different coupling strengths η. One can see that in the weak-coupling regime (e.g., $\eta = 0.15$), $F_{\rm av}$ decays monotonically and approaches to its limiting value 2/3 only when $\omega_0 t \to \infty$. If one enlarges the coupling strength moderately (e.g., $\eta = 0.35$), the strong non-Markovian effect dominates and this leads to an obvious oscillation of $F_{\rm av}$, but in the long-time limit it still reaches the classical limiting value 2/3. If one further increases the coupling strength to a much larger value (e.g., $\eta = 0.9$), however, $F_{\rm av}$ firstly experiences some oscillations, and then approaches to a finite value larger than 2/3 in the long-time limit.

To understand the physical mechanism responsible for the above phenomena, we plot in the inset of Fig. 2 the behaviors of the normalized decay rate $\gamma(t)$. Clearly, for $\eta = 0.15$ the decay rate maintains a finite value after one oscillation, and thus deprives the quantum advantage of the teleportation protocol in the long-time limit. For $\eta = 0.9$, however, $\gamma(t)$ approaches zero after some oscillations due to the energy and/or information exchanging back and forth between the qubits and their independent memory reservoirs, and this leads to $F_{\rm av} > 2/3$ even in the long-time limit. The origin of $F_{\rm av}(t \to \infty) > 2/3$ for $\eta = 0.9$ can also be explained from the formation of the bound state in the system. In fact, for the Hamiltonian model of Eq. (3) with the spectral densities of the form of Eq. (6), the conditions for formation of a bound state can be determined as

$$\eta > \begin{cases} \dfrac{\omega_0}{(s-1)!\omega_c} & (s \in \mathbb{Z}), \\ \dfrac{\omega_0}{\sqrt{\pi}\omega_c} & (s = 1/2), \end{cases} \tag{14}$$

by the same methodology of Ref. [32]. For the system parameters chosen in Fig. 2 (i.e., $s = 3$ and $\omega_c = \omega_0$), $\eta = 0.9$ is clearly larger than its critical value 0.5, and

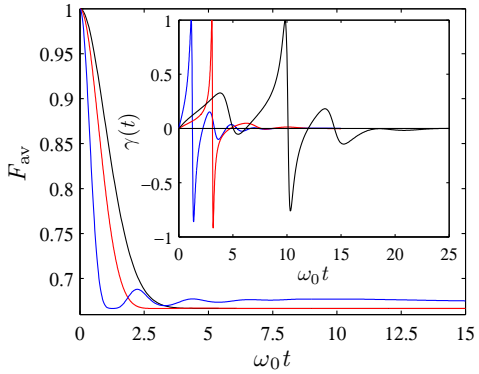

FIG. 4: (Color online) Average fidelity $F_{\rm av}$ versus $\omega_0 t$ in the sub-Ohmic reservoir with $\omega_c = \omega_0$, $r = 1$, and $\eta = 0.3$ (black), 0.55 (red), 2.1 (blue). The inset shows behaviors of the corresponding normalized decay rates $\gamma(t)$.

therefore $F_{\rm av}(t \to \infty) > 2/3$. For $\eta = 0.15$ and 0.35, which are smaller than 0.5 and thus $F_{\rm av}(t \to \infty) = 2/3$, although there may be weak enhancement of $F_{\rm av}$ (e.g., $\eta = 0.35$) during certain $\omega_0 t$ regions caused by the non-Markovian effects.

When considering the Ohmic (Fig. 3) and sub-Ohmic (Fig. 4) reservoirs, similar phenomena are observed (the oscillating behaviors of $F_{\rm av}$ for the Ohmic reservoir with $\eta = 0.9$ and sub-Ohmic reservoir with $\eta = 0.55$ are very weak and unobvious in the plots), with however different critical coupling strengths for the formation of a bound state. This corroborates the observation derived for the case of super-Ohmic reservoir.

To further understand the relations between dynamical behaviors of $F_{\rm av}$ and $\gamma(t)$, we reexamine Eq. (11), from which one can derive $\Gamma(t) = -\dot{q}(t)/q(t)$, with $q(t) = |p(t)|^2$. Therefore $\gamma(t) > 0$ when $|p(t)|$ decreases with time, and $\gamma(t) < 0$ when $|p(t)|$ increases with time. As $F_{\rm av}$ is a monotonic increasing function of $|p(t)|^2$ in the region of $|p|^2 > |p|_c^2 = (1-r)/(1+r)$, $F_{\rm av}$ is increased whenever $\gamma(t) < 0$, and decreased whenever $\gamma(t) > 0$

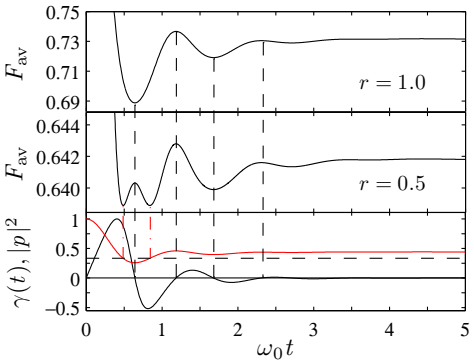

FIG. 5: (Color online) Comparison of the behaviors of $F_{\rm av}$ with that of the normalized decay rate $\gamma(t)$ (black) and the population parameter $|p(t)|^2$ (red) in super-Ohmic reservoir with $\omega_c = \omega_0$ and $\eta = 0.9$. The horizontal dashed line represents constant 1/3.

during this region. In the region of $|p|^2 < |p|_c^2$, however, $F_{\rm av}$ is a monotonic decreasing function of $|p(t)|^2$, thus $F_{\rm av}$ is decreased whenever $\gamma(t) < 0$, and increased whenever $\gamma(t) > 0$. But it should be note that for this case (i.e., $|p|^2 < |p|_c^2$), $F_{\rm av}$ cannot be larger than its classical limiting value 2/3.

In Fig. 5 we gave an exemplified plot of the time dependence of $F_{\rm av}$ and $\gamma(t)$ certifying explicitly the above general arguments. When $r = 1$, as mentioned above, $F_{\rm av}$ behaves as a monotonic increasing function of $|p(t)|^2$ in the whole time region, thus it is increased when $\gamma(t) < 0$ and decreased when $\gamma(t) > 0$. For $r = 0.5$ we have $|p|^2 < |p|_c^2 = 1/3$ during the time region $\omega_0 t \in (0.49, 0.84)$, and from the solid red line shown in Fig. 5, one can see obviously that $F_{\rm av}$ is decreased if $\gamma(t) < 0$ and increased if $\gamma(t) > 0$. As the negativity of the decay rate is a signature of strong backaction of the non-Markovian memory effect of the reservoir, the decrement of $F_{\rm av}$ with $\gamma(t) < 0$ indicates that the back flow of information from the environment to the channel does not always improve quality of teleportation.

IV. SUMMARY

In summary, we have studied quantum teleportation of a general one-qubit state in the bosonic structured reservoirs with spectral densities of the super-Ohmic, Ohmic and sub-Ohmic types. Through comparing dynamical behaviors of the average teleportation fidelity $F_{\rm av}$ with different system-reservoir parameters, we show that the structures of the reservoirs play a decisive role on quality of teleportation, and $F_{\rm av}$ can be improved by the technique of reservoir engineering, e.g., by tuning the reservoir structures so that there are bound state formulated. We have also compared behaviors of $F_{\rm av}$ with that of the decay rate $\gamma(t)$, and revealed the relationships between the negativity/positivity of $\gamma(t)$ and the enhancement/decrement of $F_{\rm av}$.

As it is now possible to simulate and control the non-Markovian effect [14–16], we hope our results may be certified with state-of-the-art experiments, and at the same time shed some new light for exploring the relationship between non-Markovianity of the reservoir and the efficiency for performing certain quantum protocols.

ACKNOWLEDGMENTS

This work was supported by NSFC (11205121, 11174165, 11275099), and the Scientific Research Program of Education Department of Shaanxi Provincial Government (12JK0986).

[1] C. H. Bennett, G. Brassard, C. Crépeau, R. Jozsa, A. Peres, W. K. Wootters, Phys. Rev. Lett. **70**, 1895 (1993).
[2] J. Lee, M. S. Kim, Phys. Rev. Lett. **84**, 4236 (2000).
[3] G. Bowen, S. Bose, Phys. Rev. Lett. **87**, 267901 (2001).
[4] F. Verstraete, H. Verschelde, Phys. Rev. Lett. **90**, 097901 (2003).
[5] Y. Yeo, W. K. Chua, Phys. Rev. Lett. **96**, 060502 (2006).
[6] M. L. Hu, H. Fan, Phys. Rev. A **86**, 032338 (2012).
[7] M. L. Hu, Ann. Phys. (NY) **327**, 2332 (2012).
[8] D. Bouwmeester, J. W. Pan, K. Mattle, M. Eibl, H. Weinfurter, A. Zeilinger, Nature **390**, 575 (1997).
[9] M. A. Nielsen, E. Knill, R. Laflamme, Nature **396**, 52 (1998).
[10] A. Furusawa, J. L. Sørensen, S. L. Braunstein, C. A. Fuchs, H. J. Kimble, E. S. Polzik, Science **282**, 706 (1998).
[11] S. Olmschenk, D. N. Matsukevich, P. Maunz, D. Hayes, L. M. Duan, C. Monroe, Science **323**, 486 (2009).
[12] J. Yin, J. G. Ren, H. Lu, et al., Nature **488**, 185 (2012).
[13] X. S. Ma, T. Herbst, T. Scheidl, et al., Nature **489**, 269 (2012).
[14] M. P. Almeida, F. de Melo, M. Hor-Meyll, A. Salles, S. P. Walborn, P. H. Souto Ribeiro, L. Davidovich, Science **316**, 579 (2007).
[15] J. S. Xu, X. Y. Xu, C. F. Li, C. J. Zhang, X. B. Zou, G. C. Guo, Nature Commun. **1**, 7 (2010) .
[16] B. H. Liu, Y. F. Huang, C. F. Li, G. C. Guo, E. M. Laine, H. P. Breuer, J. Piilo, Nature Phys. **7**, 931 (2011).
[17] L. Mazzola, J. Piilo, S. Maniscalco, Phys. Rev. Lett. **104**, 200401 (2010).
[18] M. L. Hu, H. Fan, Ann. Phys. (NY) **327**, 851 (2012).
[19] M. L. Hu, H. Fan, Ann. Phys. (NY) **327**, 2343 (2012).
[20] S. Oh, S. Lee, H.W. Lee, Phys. Rev. A **66**, 022316 (2002).
[21] E. Jung, M. R. Hwang, Y. H. Ju, et al., Phys. Rev. A **78**, 012312 (2008).
[22] D. D. Bhaktavatsala Rao, P. K. Panigrahi, C. Mitra, Phys. Rev. A **78**, 022336 (2008).
[23] M. L. Hu, Phys. Lett. A **375**, 922 (2011).

[24] M. L. Hu, Phys. Lett. A **375**, 2140 (2011).
[25] M. L. Hu, J. Phys. B **44**, 025502 (2011).
[26] M. L. Hu, J. Phys. B **44**, 095502 (2011).
[27] Y. Yeo, Z. W. Kho, L. Wang, Europhys. Lett. **86**, 40009 (2009).
[28] M. L. Hu, Eur. Phys. J. D **64**, 531 (2011).
[29] A. J. Leggett, S. Chakravarty, A. T. Dorsey, M. P. A. Fisher, A. Garg, W. Zwerger, Rev. Mod. Phys. **59**, 1 (1987).
[30] R. Horodecki, M. Horodecki, and P. Horodecki, Phys. Lett. A **222**, 21 (1996).
[31] H.-P. Breuer, F. Petruccione, *The Theory of Open Quantum Systems* (Oxford University Press, Oxford, 2002).
[32] Q. J. Tong, J. H. An, H. G. Luo, C. H. Oh, J. Phys. B **43**, 155501 (2010).
[33] B. Bellomo, R. Lo Franco, G. Compagno, Phys. Rev. Lett. **99**, 160502 (2007).
[34] R. F. Werner, Phys. Rev. A **40**, 4277 (1989).